Asociación Argentina
de Mecánica Computacional

Mecánica Computacional Vol XXIX, págs. 5303-5319 (artículo completo)
Eduardo Dvorkin, Marcela Goldschmit, Mario Storti (Eds.)
Buenos Aires, Argentina, 15-18 Noviembre 2010

NUMERICAL SIMULATIONS OF RATE/TIME EFFECTS IN CONCRETE

Ricardo H. Lorefice[a], Guillermo Etse[b] and Marcia Rizo Patron[a]

[a]*Centro de Mecánica Aplicada y Estructuras, Universidad Nacional de Santiago del Estero, Avda. Belgrano (S) 1912, 4200 Santiago del Estero, Argentina, rlorefice@gmail.com,*

[b]*Centro de Métodos Numéricos y Computacionales en Ingeniería, Universidad Nacional de Tucumán Avda. Roca 1800, 4000, San Miguel de Tucumán, Argentina, getse@herrera.unt.edu.ar,*

Keywords: Rate/Time Effects, Numerical Simulations, Concrete.

Abstract. Structural response of concrete strongly depends on the nature of applied loads. Time varying loads can induce rate/time effects in concrete like increasing strength (rate effect) or basic creep deformation (under sustained loads). In this paper we present a computational approach that numerically simulates concrete mesostructure like a two-phase material. Each material phase is represented by continuum and interface finite elements which allow to track the crack trajectories under different loading scenarios. A specific rate-dependent interface constitutive law is included in the model in order to capture the rate/time effects and their incidence in the global structural response of the specimen.

AMCA http://www.amcaonline.org.ar.

1 INTRODUCTION

Since several decades concrete has been used as structural material in the field of civil engineering. It is then clear the necessity of an adequate understanding of its behavior under load. Many researchers have studied and still study concrete from both experimental and theoretical point of view. Nevertheless the mechanical behavior of concrete is still not completely understood especially as far as cracking and failure are involved. The heterogeneity coming from the coupling between aggregate and cement paste leads to a non uniform distribution of the applied load in the internal mesostructure of concrete material. This lack of homogeneity in turn implies a gradual localization of deformation and material rupture. Cracking localization is the main reason of the large number of different responses given by concrete under different loading conditions. Despite the complexity of static concrete response, a significant effort has been made to properly capture rate/time effects in concrete materials. Several authors studied both aspects of material behavior, but always focusing on one of those topics at time, and frequently at macro-level of observation, by considering phenomenological constitutive models. In the last years, the increasing capacity of modern digital computers allows analyzing computational problems at different levels of observation, generally with an increasing problem size when the scale becomes smaller. In this work we present an integrated approach to face the rate/time concrete sensitivity problem by using the Finite Element Technique at meso-level of observation. This approach is characterized by inserting interface finite elements (zero-thickness-four node finite elements or joint elements) between the edges of conventional finite elements to represent potential crack lines following Hillerborg's *Fictitious Crack Model* (1976) in order to properly account fracture behavior, detection of explicit crack paths, aggregate-mortar phases interaction and energy dissipation of concrete and cementitious materials under static and dynamic loading scenarios. Here, the term "dynamic" means that the proposed model is capable to take into account different loading velocities or loading rates, and also the relaxation/creep behavior under sustained loads by using a unique visco-elastoplastic constitutive law at the interfaces, which allows to run computer simulations of both quasi-static and rate/time loading cases using an integrated approach.

2 VISCOELASTOPLASTIC LAW FOR ENGINEERING MATERIALS

In order to take into account rate/time effects, several models has been proposed, see a.o. Duvaut & Lions (1972), Bodner & Partom (1972), Perzyna (1963), (1966). For engineering materials, the most widely accepted rate-dependent constitutive theory is the Perzyna's type elasto-viscoplastic material formulation. The main feature of this model is that the rate-independent yield function used for describing the viscoplastic strain can become larger than zero, which effect is known as "*overstress*", see Figures 1 and 2. The characteristics of the Perzyna model have been addressed by several authors, see a.o. Simo (1989), Sluys (1992), Wang (1997), Simo & Hughes, (1998), Etse & Willam (1999), Carosio et al. (2001), Etse & Carosio (2002). Restricting our analysis to the small-strain case, the total strain rate $\dot{\boldsymbol{\varepsilon}}$ can be decoupled into an elastic and a viscoplastic part which accounts for both irreversible and viscous deformation,

$$\boldsymbol{\varepsilon} = \boldsymbol{\varepsilon}_e + \boldsymbol{\varepsilon}_{vp} \tag{1}$$

Like in classical elasto-plasticity theory, the stress rate $\dot{\boldsymbol{\sigma}}$ is related to the strain rate by the

constitutive relation

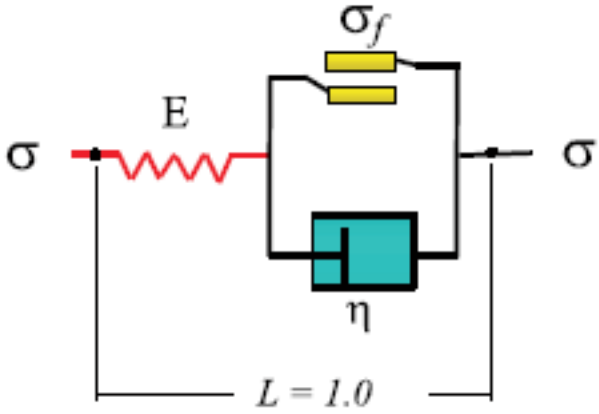

Figure 1: Perzyna's elasto-viscoplastic rheological device

$$\dot{\boldsymbol{\sigma}} = \dot{\boldsymbol{\sigma}}_e - \dot{\boldsymbol{\sigma}}_{vp} = \mathbf{E} : (\dot{\boldsymbol{\varepsilon}} - \dot{\boldsymbol{\varepsilon}}_{vp}) \tag{2}$$

The evolution of the viscoplastic strain rate is defined as (Perzyna, 1966)

$$\boldsymbol{\varepsilon}_{vp} = \mathbf{g}(\psi, F, \boldsymbol{\sigma}) = \frac{1}{\eta}\langle \psi(F) \rangle \mathbf{m} \tag{3}$$

$$\mathbf{m} = \mathbf{A} : \mathbf{n} = \mathbf{A} : \frac{\partial F}{\partial \boldsymbol{\sigma}} \tag{4}$$

with $\psi(F)$ a dimensionless monotonically increasing over-stress function, η the viscosity parameter and **m** the viscoplastic potential gradient defined as a modification of the gradient tensor **n** of the yield surface F by means of the fourth order transformation tensor ***A***. In this work, the following widely-used expression for $\psi(F)$ is adopted, see a.o. Simo (1989), Sluys (1992), Wang *et al.* (1997), Simo & Hughes (1998), Etse & Willam (1999)

$$\psi(F) = \left[\frac{F(\boldsymbol{\sigma}, \mathbf{q})}{F_0} \right]^N \tag{5}$$

In equation (5), $F = F(\boldsymbol{\sigma}, \mathbf{q})$ is a convex yield function which defines the limit of the elastic domain, F_0 is a normalizing factor, usually chosen equal to the initial yield limit and N a constant defining the order of the Perzyna's viscoplatic formulation. Higher values of the exponent N leads to more rate-sensitive models, while the McCauley brackets in Equation (3) defines the features of the over-stress function as

$$\langle \psi(F) \rangle = \begin{cases} F & \text{if } F > 0 \\ 0 & \text{if } F \leq 0 \end{cases} \tag{6}$$

The evolution law for the set of hardening/softening variables **q** is defined as

$$\dot{\mathbf{q}} = \frac{1}{\eta}\langle \psi(F) \rangle \mathbf{H} : \mathbf{m} \tag{7}$$

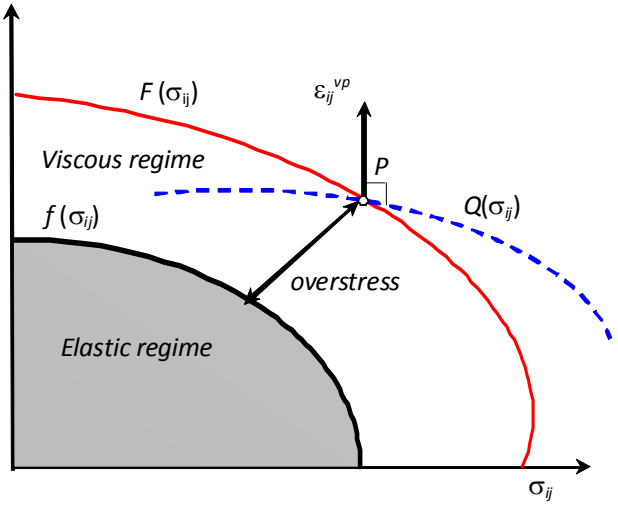

Figure 2: Over-stress concept in stress space

being ***H*** a suitable tensorial function of the state variables. In the continuous formulation, the previous set of equations is complemented by a consistency parameter $\dot{\lambda}$, defined as an increasing function of the over-stress

$$\dot{\lambda} = \frac{\langle \psi(F) \rangle}{\eta} \tag{8}$$

The evolution equations (3) and (7) can be expressed quite similar to elasto-plasticity theory as

$$\dot{\boldsymbol{\varepsilon}}_{vp} = \dot{\lambda}\mathbf{m} \tag{9}$$

$$\dot{\mathbf{q}} = \dot{\lambda}\mathbf{H} : \mathbf{m} = \dot{\lambda}\mathbf{h} \tag{10}$$

being $\mathbf{h} = \boldsymbol{H}:\mathbf{m}$. From equations (3) and (9) follows (Ponthot (1995), Etse and Willam (1999))

$$F = \psi^{-1}\left(\frac{\|\boldsymbol{\varepsilon}_{vp}\|}{\|\mathbf{m}\|}\eta\right) = \psi^{-1}(\dot{\lambda}\eta) \tag{11}$$

The new constraint condition, valid to the viscoplastic range takes now the form

$$\bar{F} = F - \psi^{-1}(\dot{\lambda}\eta) = 0 \tag{12}$$

Equation (12) can be viewed like a generalization of the inviscid yield condition *F=0* for rate-dependent Perzyna type materials. The name *continuous formulation* is due to the fact that the condition $\eta = 0$ (without viscosity effect) leads to the elastoplastic yield condition *F=0*. Moreover, from equation (8) follows that when $\eta \to 0$ the consistency parameter remains finite and positive since also the over-stress goes to zero. The other extreme case, $\eta \to \infty$ leads to the inequality $\bar{F} < 0$ for every possible stress state, indicating that only elastic response may be activated. The constraint condition defined by equation (12) allows a generalization of the Kuhn-Tucker conditions which may be now written as

$$\dot{\lambda}\bar{F} = 0 \qquad \dot{\lambda} \geq 0 \qquad \bar{F} \leq 0 \tag{13}$$

Finally, the viscoplastic consistency condition expands into

$$\dot{\bar{F}} = \mathbf{n} : \dot{\boldsymbol{\sigma}} + \bar{r}\dot{\lambda} + \bar{s}\ddot{\lambda} = 0 \tag{14}$$

where

$$\bar{r} = \frac{\partial \bar{F}}{\partial q} = \frac{\partial F}{\partial q} - \frac{\partial \psi^{-1}(\dot{\lambda}\eta)}{\partial q} \tag{15}$$

and

$$\bar{s} = -\frac{\partial \varphi^{-1}(\eta\dot{\lambda})}{\partial \dot{\lambda}} \tag{16}$$

3 RATE DEPENDENT INTERFACE MODEL

In this section the rate-dependent extension of the interface model by Carol *et al* (1997) , and Lopez (1999) is summarized. The viscoplastic yield condition for the interface constitutive model can be expressed as

$$\bar{F} = \sigma^2 - (c - \tau tg\phi)^2 + (c - \chi tg\phi)^2 - (\dot{\lambda}\eta)^{1/N} \tag{17}$$

being σ and τ the normal and tangential stress components at the interface with χ the traction strength (vertex of hyperbola), c the apparent cohesion (shear strength) and ϕ the friction angle. The energy dissipated during the time-dependent fracture process is defined as

$$dW^{vcr} = \sigma\, du^{vcr} + \tau dv^{vcr} \quad \text{if } \sigma \geq 0 \tag{18}$$

$$dW^{vcr} = \tau dv^{vcr}\left(1 - \left|\frac{\sigma \mathrm{tg}\phi}{\tau}\right|\right) \quad \text{if } \sigma < 0 \tag{19}$$

Whereby u^{vcr} and v^{vcr} are the normal and tangential (critical) rate-dependent rupture displacements, respectively. The viscoplastic flow is fully associated in tension while non-associated in compression, according to

$$\mathbf{m} = \mathbf{A} : \mathbf{n} \tag{20}$$

$$\mathbf{n} = \frac{\partial F}{\partial \boldsymbol{\sigma}} = \begin{bmatrix} \dfrac{\partial F}{\partial \sigma} \\ \dfrac{\partial F}{\partial \tau} \end{bmatrix} = \begin{bmatrix} 2tg\phi(c - \sigma tg\phi) \\ 2\tau \end{bmatrix} \tag{21}$$

$$\mathbf{A} = \begin{bmatrix} 1 & 0 \\ 0 & 1 \end{bmatrix} \quad \text{if } \sigma > 0 \tag{22}$$

and

$$\mathbf{A} = \begin{bmatrix} f_\sigma^{dil} f_c^{dil} & 0 \\ 0 & 1 \end{bmatrix} \quad \text{if } \sigma < 0 \tag{23}$$

being **A** a (2x2) transformation matrix, **n** the gradient to the viscoplastic yield surface and **m** the gradient to the viscoplastic potential function. The factors f_c^{dil} and f_σ^{dil} accounts for the dilatancy effects in the compressive regime by means of a reduction of the normal component σ. The continuum viscoplasticity form of the rate dependent interface constitutive model is defined by the following set of equations:

$$\dot{\mathbf{u}} = \dot{\mathbf{u}}^e + \dot{\mathbf{u}}^{vcr} \tag{24}$$

$$\dot{\mathbf{u}}^e = \left(\mathbf{E}\ \right)^{-1} \dot{\boldsymbol{\sigma}} \tag{25}$$

$$\dot{\boldsymbol{\sigma}} = \mathbf{E}(\dot{\mathbf{u}} - \dot{\mathbf{u}}^{vcr}) \tag{26}$$

where $\dot{\mathbf{u}}$ are the rate of the relative displacements which are decomposed into an elastic $\dot{\mathbf{u}}^e$ and a viscoplastic component $\dot{\mathbf{u}}^{vcr}$, **E** is the 2x2 elastic stiffness matrix which has a diagonal structure with non-zero terms equal to the constant assumed normal and shear stiffness $E_N = E_T$. The non-linear system of equations is solved using a Newton-Raphson iterative procedure in the framework of the Closest Point Projection Method (CPPM) starting from the expansion of a Taylor's series truncated at the first term, see Etse et al (1999), (2000), (2002), Lorefice (2007)

$${}^{i}\dot{\bar{F}} = {}^{i-1}\dot{\bar{F}} + {}^{i-1}\left(\frac{d\bar{F}}{d\Delta\lambda}\right) {}^{i}d\Delta\lambda = 0 \tag{27}$$

from equation (27), the differential change in the elasto-viscoplastic multiplier is derived as

$${}^{i}d\Delta\lambda = -{}^{i-1}\dot{\bar{F}} \left[{}^{i-1}\left(\frac{d\bar{F}}{d\Delta\lambda}\right) \right]^{-1} \tag{28}$$

Assuming the hypothesis: $d\dot{\lambda} = d\Delta\lambda / \Delta t$, see Ponthot (1995), Wang (1997), Carosio & Etse (2001), the derivative of the viscoplastic yield function respect to $\Delta\lambda$ takes now the form

$$\frac{d\bar{F}}{d\Delta\lambda} = \mathbf{n}^T \left(\frac{\partial \boldsymbol{\sigma}}{\partial \Delta\lambda}\right) + \left(\frac{dF}{dc}\frac{dc}{d\dot{W}^{vcr}} + \frac{dF}{d\chi}\frac{d\chi}{d\dot{W}^{vcr}}\right)\left(\frac{d\dot{W}^{vcr}}{d\mathbf{u}^{vcr}}\right)^T \mathbf{m} - \frac{\eta}{\Delta t} \tag{29}$$

Considering $d\boldsymbol{\sigma} / d\Delta\lambda = -\mathbf{E}^m \mathbf{m}$, with

$$\mathbf{E}^m = (E^{-1} + \Delta\lambda \mathbf{M}) \tag{30}$$

whereby $\mathbf{E}^m$ is the modified elastic matrix and $\mathbf{M} = \partial \mathbf{m} / \partial \boldsymbol{\sigma}$ the Hessian matrix for the interface model

$$\mathbf{M} = \begin{bmatrix} -2tg^2\phi & 0 \\ 0 & -2 \end{bmatrix} \tag{31}$$

Replacing the differential stress change with respect to $\Delta\lambda$ into equation (29), the expression for $d\Delta\lambda$ results

$$^{i}d\Delta\lambda = -\frac{^{i-1}\overline{F}}{\left[-\mathbf{n}^T\mathbf{E}^m\mathbf{m} + \left(\frac{dF}{dc}\frac{dc}{d\dot{W}^{vcr}} + \frac{dF}{d\chi}\frac{d\chi}{d\dot{W}^{vcr}}\right)\left(\frac{d\dot{W}^{vcr}}{d\mathbf{u}^{vcr}}\right)^T\mathbf{m} - \frac{\eta}{\Delta t}\right]} \tag{32}$$

from where the increments of the stress vector and state variables can be obtained.

4 DYNAMIC AND RHEOLOGICAL CONCRETE BEHAVIOR

4.1 Rate / time effects in concrete

Frequently, concrete behavior is treated as rate/time-independent material. This approach is acceptable only as an approximation. To analyze the structural response of real structures, the rate/time-dependent phenomenon in concrete must be considered and included in the structural model. Time dependence is negligible in a certain range of load duration referred as short term (static) loading and pertaining to usual material tests lasting few hours. On the contrary it is important for dynamic (impact) loading lasting few milliseconds and for long-term (sustained) loading lasting many years, see Figure 3.

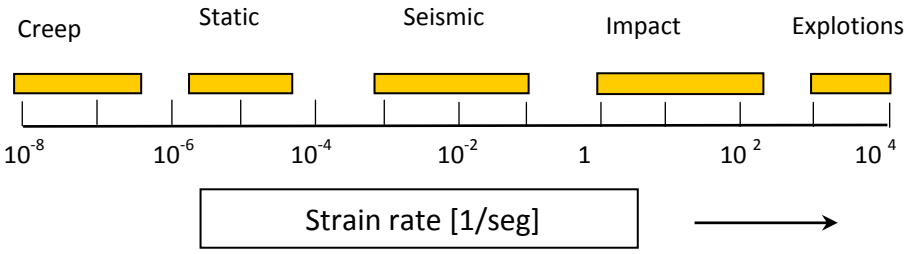

Figure 3: Strain rate under several loading cases (Bischoff & Perry, 1991)

Under impact loading the influence of the loading rate on concrete behavior becomes an important parameter that must be taken into account in order to have reasonable results. It is generally reported that when the strain rate increases, the ultimate stress, the elastic (secant) modulus and the peak strain increase, whereas the apparent Poisson's ratio and the post-peak slope branch decrease, becoming more steeper, brittle response. For concrete, the strain rate effect on peak strength is larger under tensile loads than when subjected to compressive loads, see Figure 4. On the other hand, under sustained loading concrete shows creep and visco-elastoplastic deformations develop even at constant load, see Figures 5 and 6. It should be remarked that creep is a very challenging problem because it is influenced by many factors. The age of loading, the temperature and the water content (humidity) which in turn depends on the environmental conditions, strongly affect creep. Attainment of a satisfactory understanding of the physical mechanism has defied seven decades of determined research

efforts. Initially, the aging and the environmental effect were simply described by empirical functions. However, the test data are highly scattered and cover a limited range of conditions. Therefore, a model with reliable prediction capabilities can be formulated and identified from the data only if it is based on a good, physically justified theory.

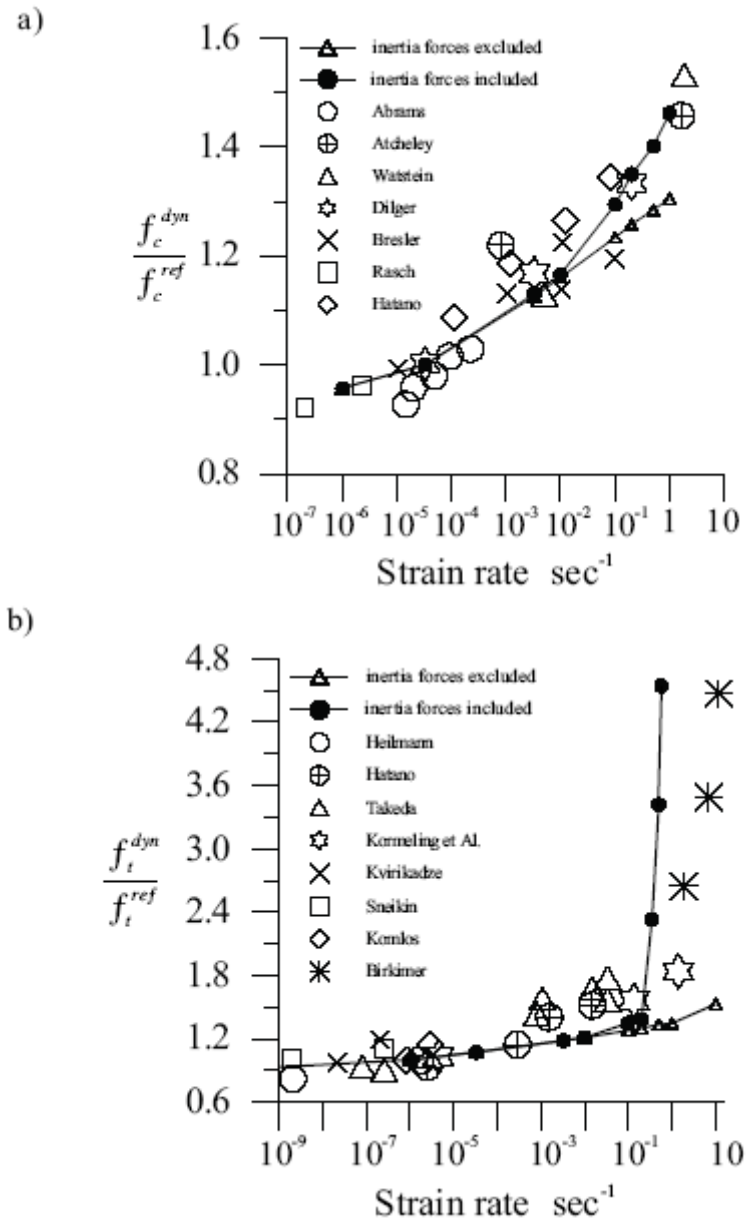

Figure 4: Rate effect on concrete strength. Comparison between numerical - experimental results: a) Compressive strength. b) Tensile strength.

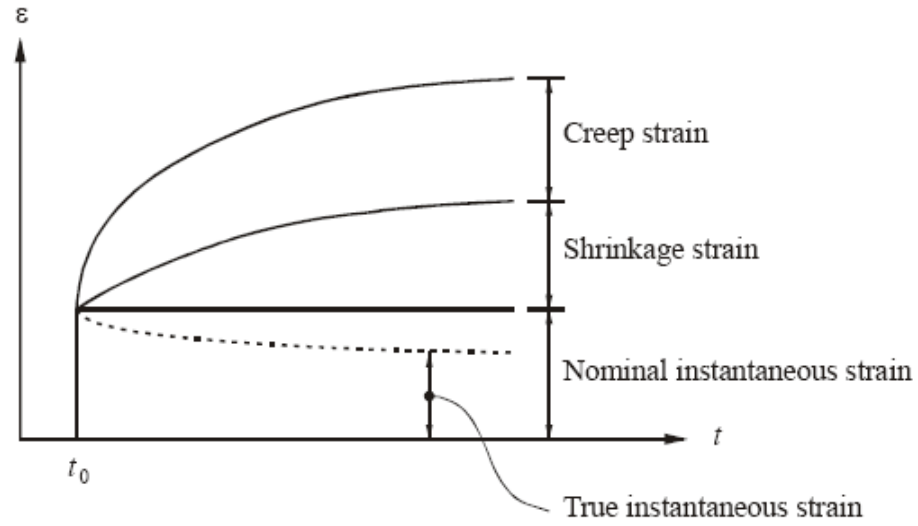

Figure 5: Time dependent strains in concrete (shrinkage and creep strain under sustained load)

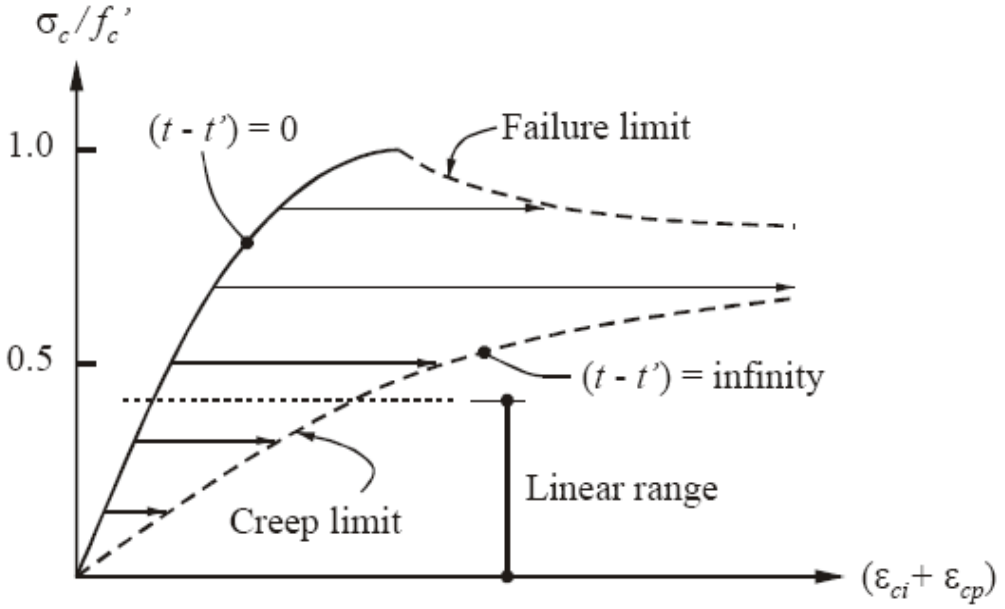

Figure 6: Influence of stress level and sustained duration on concrete mechanical strain
ε_{ci}: instantaneous strain; ε_{cp}: creep strain (Gilbert, 1988)

4.2 Concrete fracture as a rate/time dependent phenomenon

As verified experimentally, the rate dependence of concrete deformations is originated by two different physical mechanisms. The first one is a dependence of the fracture process on the rate of crack opening, and the second is the viscoelastoplastic deformation of cement paste. For concrete both mechanisms are important but the former dominates at extreme strain rates under impact. Moreover also for moderate strain rates concrete creep (material viscous deformation) would be insufficient to describe some recent findings. It has been shown that concrete exhibits a reversal of softening into hardening after a sudden increase of the loading rate (Bazant et al. 1995; Bazant and Gettu 1992; Tandon et al. 1995). The strain rate influences also the fracture properties of concrete as well as its strength. According to experimental data by Bazant and Gettu (1992), the fracture energy increases for increasing loading rate. It is interesting to note that these findings implies the change of the characteristic

lengths for the different tests, with a decrease of the characteristic length for increasing rate of loading, see Wittmann (1984). As showed by Tandon et al (1995), concrete response is sensitive also to sudden changes (increase or decrease) of the loading rate.

5 NUMERICAL SIMULATIONS

5.1 Rate effects

In order to illustrate model performance under different loading scenarios, we consider the patch of elements illustrated in Figure 7. This configuration allows investigating rate/time effects isolating the interface response from complex boundary conditions and mesh issues. For numerical simulations of rate effects a constant displacement rate is applied at the top nodes of the patch, while for time effects a sustained load or fixed displacement is imposed.

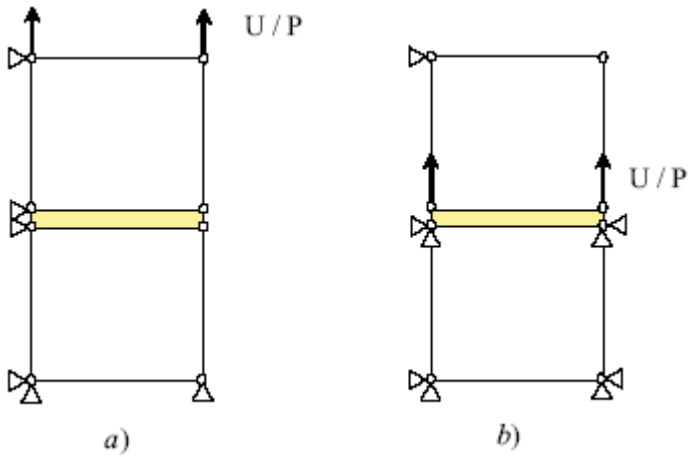

Figure 7: Continuum and interface element arrangement for rate/time effects

Numerical simulations are carried-out imposing a constant displacement rate (normal displacements) at the top nodes of the interface (configuration *b)* in Figure 7). Figure 8 illustrate normal stress response under traction loads for different velocities for the following interface data set: E_N=10000 MPa/m, χ_0=2.0 MPa, G^I_f = 0.03 N/mm, G^{II}_f=10G^I_f and rest of parameters equal to zero. The apparent viscosity η =1.E6 MPa.seg, the time step and Perzyna's exponent: dt = 5.E-3 sec and N=1 respectively. The range of displacement rate varies between 2.E-5 - 1.E-3 m/sec. The continuum elements are characterized by E =25000 MPa and v =0.2. For increasing loading rates the peak strength increase, tending to the elasto-plastic response when the displacement rate goes to zero, recovering the inviscid response. The influence of Perzyna's exponent N in model response is presented in Figure 9, running numerical simulations for a fixed displacement rate 2.E-4 m/sec. As explained before, for increasing N values a more rate-sensitive formulation is obtained. The capability of the constitutive model to reproduce the experimental findings of Bazant and Gettu (1992), and Tandon et al (1995) were verified by imposing a sudden change (increase/decrease) in the loading rate at a point P located on the post-peak softening branch. In both cases the effect is properly captured, which is verified by the coincidence of the corresponding curves for the higher/lower velocities regarding the reference (central) curve test. In the case of a sudden increase in the displacement rate, the post-peak softening reverses to post-peak hardening followed by a second peak. Afterwards the curve coincides with the corresponding monotonic

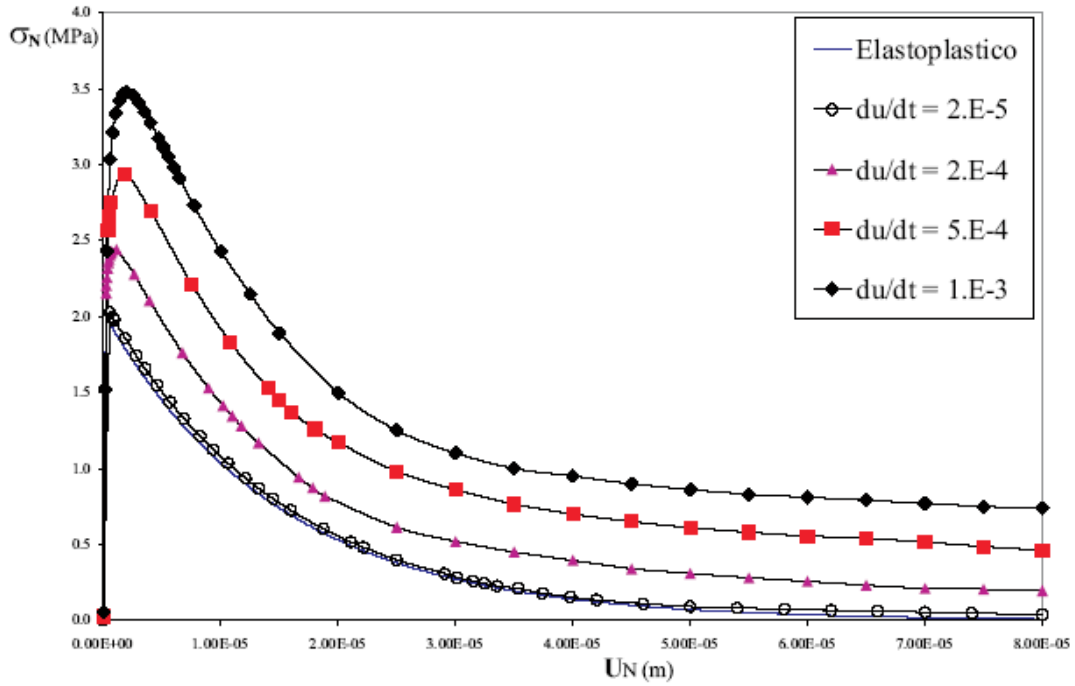

Figure 8: Model response for different velocities – uniaxial traction test

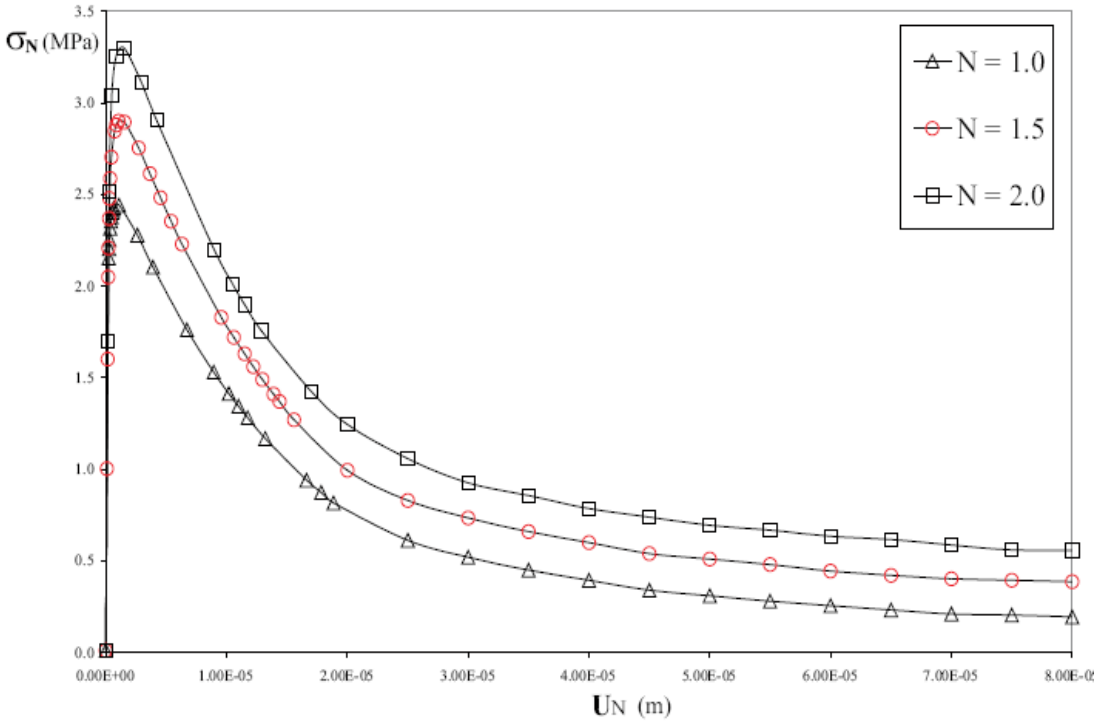

Figure 9: Model response for different velocities – uniaxial traction test

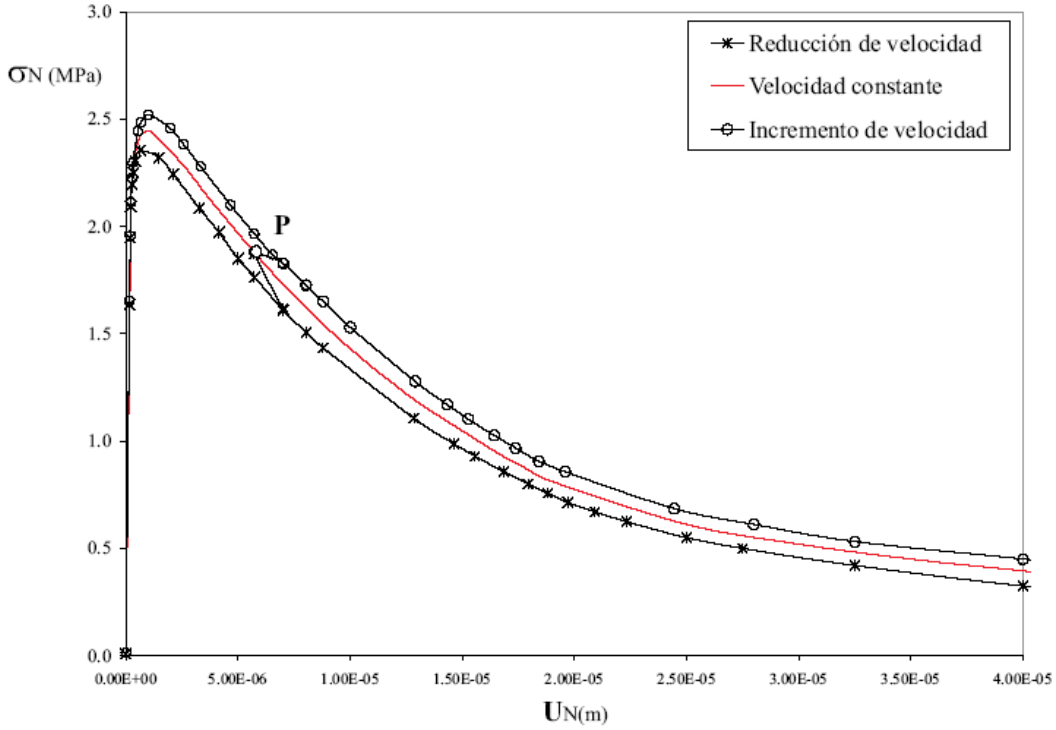

Figure 10: Numerical simulation - reversal of softening effect

curve for the higher rate of loading. The second peak may be higher or lower than the first peak at the previous slow rate of loading, depending on the ratio of rate increase and the magnitude of load decrease prior to the increase of loading rate. In the case of a sudden decrease of the loading rate, the slope of the load-displacement diagram suddenly becomes steeper. A mild slope is resumed when the load-displacement curve gets the response for the lower loading rate. The obtained numerical results agree very well with the experimental findings by Tandon et al. (1995). Finally, the constitutive formulation is validated comparing model performance versus several experimental results available in the scientific literature, see Figure 11. In the framework of the viscoplastic flow theory the time dependence of the material parameters and particularly the over-strength is introduced by the apparent viscosity parameter η. To properly reproduce the complex variation of the concrete tensile over-strength with a wide range of applied loading rates, a displacement rate-dependent description of the viscosity parameter needs to be incorporated. On the basis of Suaris and Shah dynamic tensile tests (1984, 1985), the following evolution law for the viscosity parameter is proposed in terms of the applied velocity, see Lorefice et al (2008a):

$$\eta = \eta(\dot{u}) = \eta_0 \left[\alpha \ln(\dot{u}) + \beta \sqrt{\dot{u}} + \gamma \right] \tag{33}$$

Whereby $\dot{u}$ represents the displacement rate at the interface, and the coefficients are α = 0.072, β = 0.719 and γ = 1.678, while the initial viscosity is η_0 =1.E5 MPa.sec. The prediction of the interface model in terms of the tensile dynamic increase factor DIF is plotted in Figure 11 and compared versus several experimental results.

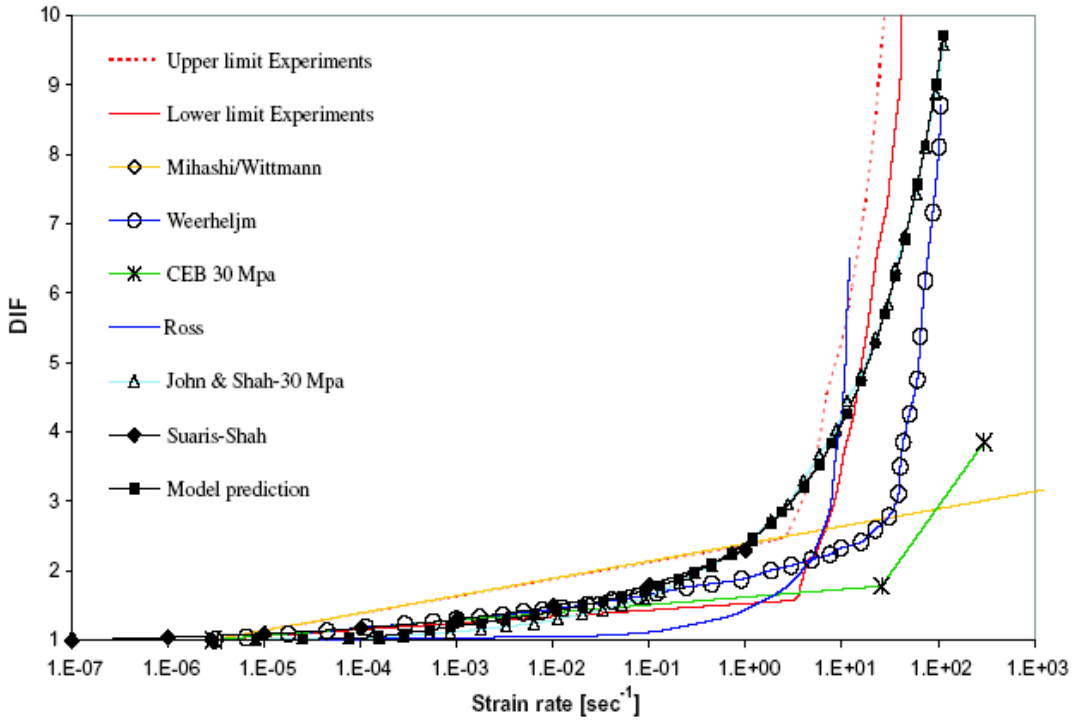

Figure 11: Dynamic increase factor in the uniaxial tensile tests.

5.2 Relaxation and basic creep tests

Model performance to simulate time dependent failure processes is illustrated by two different types of loading cases: a) A constant normal displacement is applied as showed in Figure 12 (a), which resulted to a constant strain state. The applied displacements are chosen in such a way that the corresponding internal stress state to be above the yield limit. In this case, the way that the stresses develop with respect to time is of interest. Usually such a loadcase goes by the name relaxation. (b) A constant force is applied to the top nodes of the interface element, see Figure 12 (b), which results to a constant stress state. The magnitude of the force is taken to be such, that the resulting stresses exceed the yield limit. Our interest in this case is to study the evolution of the displacements with respect to time. This model corresponds to that frequently found in the literature as basic creep case (deformation under sustained load).

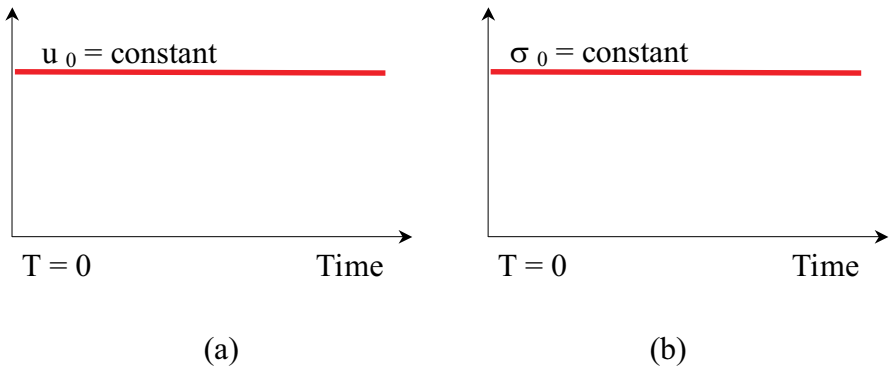

Figure 12: Constitutive tests: a) Relaxation b) Creep

In the following we will further explore the relaxation test for the following set of material parameters: E_N = 1.E7 MPa/m, χ_0 = 2.0 MPa, G_f^I = 0.00003 MPa.m, $G_f^{II} = 10G_f^I$. For these parameters the yield limit in pure traction is χ_0 = 2.0 MPa; therefore a displacement of 3.E-7 m was applied which corresponds to a uniform stress state of 3.0 MPa. The results of the elastoplastic and the elasto-viscoplastic computations are shown in Figure 13.

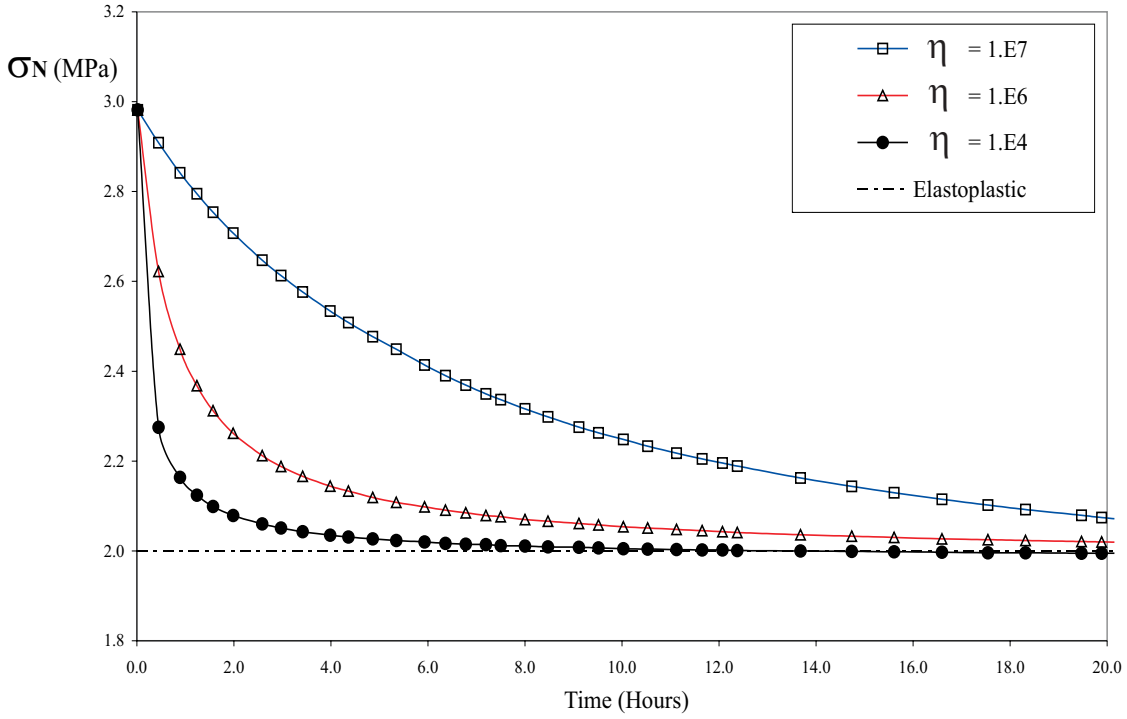

Figure 13: Relaxation test – constitutive level

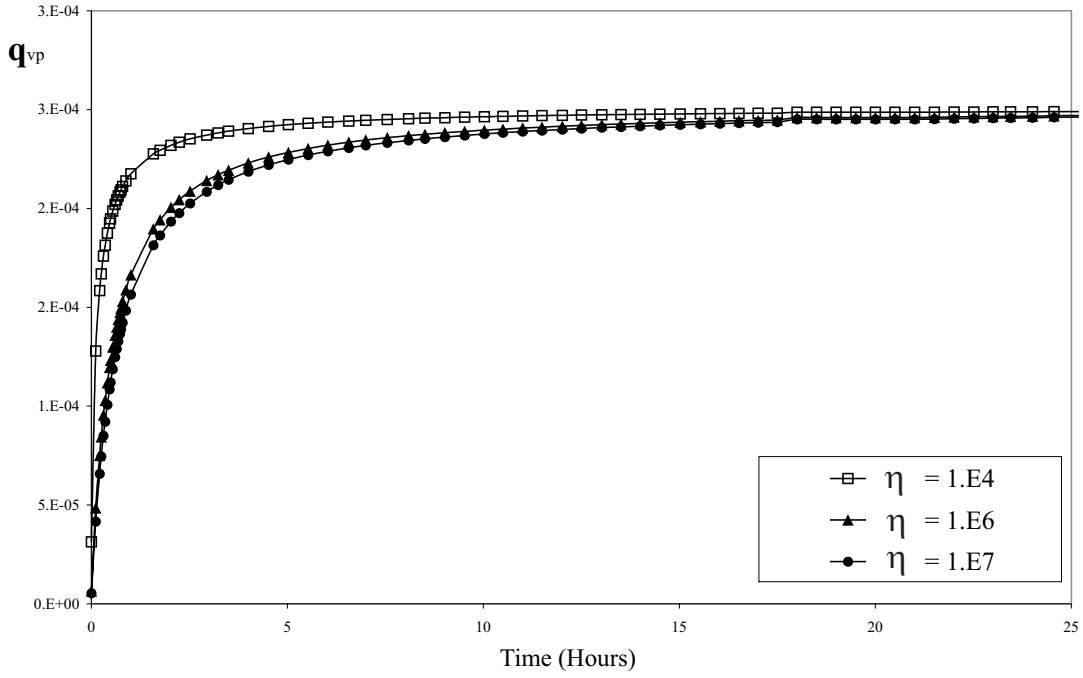

Figure 14: Relaxation test – evolution of state variable

In the same figure several cases are also plotted for different values of the viscosity parameter η. In this loadcase one may find interesting that the stresses cannot exceed the yield limit in the case of an elastoplastic material, while in the case of viscoplasticity it is in general allowed, to exceed this limit. In other words, the stresses that are developed at the interface in the case of viscoplasticity are allowed to be larger than the yield limit χ_0. This is a big advantage of viscoplasticity, since from the numerical point of view it can provide a better, more stable and reliable algorithm. From the engineering point of view it also provides a behavior coming closer to the terms, of short term and long term load carrying capacity. The evolution of the state variable is illustrated in figure 14. Also, for higher values of the viscosity parameter, higher times are needed to reach the limit value. In Figure 15 we compare the viscoelastic solution from a Maxwell chain versus the viscoplastic one for a natural relaxation time t* = η/E = 1. For this case and for comparison purposes, we introduce here two variants of the original model: a perfect viscoplastic model (with a plastic modulus $H_p = 0$), and a hardening version (setting $H_p > 0$). We can see that while for perfect viscoplasticity the numerical solution relax the stress state until reach the elastoplastic strength limit, the viscoelastic case has no limit and spread to relax the stress state to zero. Furthermore, is clear the physical meaning of the viscosity parameter η, concerning the time that the system needs to relax the stress state until reach the final, elastoplastic solution. In the same plot the hardening and softening relaxation cases are also included. Contrarily to the perfect viscoplasticity case in which the stress state evolves until reach the strength limit, for the softening/hardening cases, the stress state returns to a different stress level that depends on the value of the plastic modulus H_p.

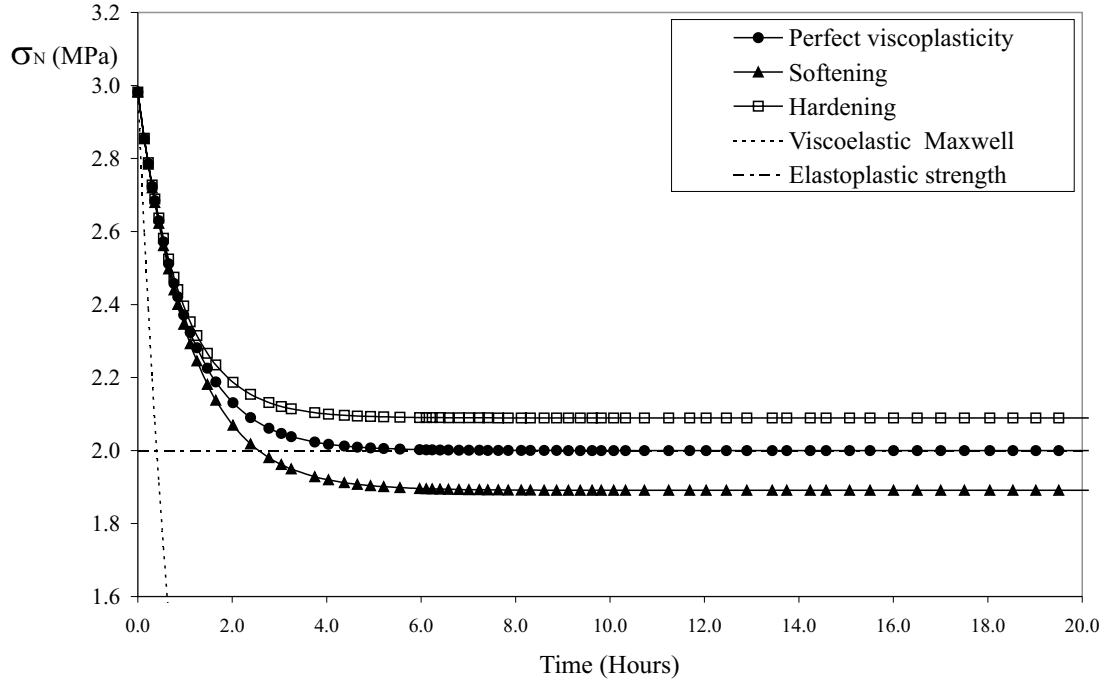

Figure 15: Comparison of different models for identical t*=η/E

6 CONCLUSIONS

A unified, integrated approach has been presented to properly analyze both, rate and time effects in concrete and cementitious materials. The proposed constitutive model is formulated on the basis of an extension of the inviscid interface model by Carol et al (1997), by introducing the Perzyna's viscoplasticity theory and the overstress concept. The resultant interface model was calibrated using a wide range of experimental results by a new rate-dependent viscosity function which allows to properly fit the experimental results under dynamic tensile loading. Model capabilities were also tested by investigating the reversal of softening effect, achieving reasonable results which qualitative agree with the available experiments by Tandon et al (1995). Finally, time-dependent problems were addressed by exploring the numerical response under creep/relaxation tests. From these results, it is clear that the proposed formulation, with a proper calibration is a very promising numerical tool to include rate/time effects in the structural analysis of real concrete structures, contributing to a better understanding of material non-linearity, capture of increasing strength under increasing strain rates, and rate-dependent post-peak concrete behavior in the velocity range that exclude inertial effects.

REFERENCES

Bazant, Z.P., Gettu, R.. Rate effects and load relaxation in static fracture of concrete. ACI Materials Journal 89 (5), 456–468, 1992.

Bischoff, P.H. and Perry, S.H., Compressive behavior of concrete at high strain rates, Material and Structures, N^0. 24, Pages. 425-450, 1991.

Bodner, S.R, and Partom, Y. Constitutive Equations for elastic-viscoplastic hardening materials. ASME Journal of Applied Mechanics.42, 385-9, 1975.

Carol, I., Prat, P. and Lopez, C.M., A Normal/Shear Cracking Model. Interface Implementation for Discrete Analysis. *Journal of Engineering Mechanics*, *ASCE*, 123(8), pp. 765-773, 1997.

Carosio, A., Viscoplasticidad Continua y Consistente. *Tesis doctoral, Laboratorio de Estructuras - Universidad Nacional De Tucumán*, Argentina, 2001.

Carosio, A., Willam, K. and Etse, G., On the Consistency of Viscoplastic Formulations. *International Journal of Solids and Structures*, Vol. 37, pp. 7349-7369, 2000.

Duvaut, G. and Lions, J.L. Les inequations en mechanique et en physique, Dunod, Paris (1972).

Etse, G., Carosio, A. and Willam, K., Limit State and Localization of Perzyna Viscoplastic Material. *Int. Journal on Cohesive and Frictional Materials,* (23), 1, pp. 32-42, 1997.

Etse, G., Willam, K., Failure Analysis of Elastoviscoplastic Material Models. *Journal of Engng. Mechanics*, (125), 1, pp. 60-69, 1999.

Etse, G., Lorefice, R., Carosio, A. and Carol, I., Rate Dependent Interface Model Formulation for Quasi-Brittle Materials. *Proc. International Conference on Fracture Mechanics of Concrete Structures - FRAMCOS 5*. Boulder, Colorado, USA, pp. 301-305, 2004.

Etse, G., Lorefice, R., López, C.M. and Carol, I., Meso and Macromechanic Approaches for Rate Dependent Analysis of Concrete Behavior. *International Workshop in Fracture Mechanics of Concrete Structures*. Vail, Colorado, USA, 2004.

Hillerborg, A, Modeer, M and Peterson, P. Analysis of crack formation and crack growth in concrete by means of fracture mechanics and finite elements, Cement Concrete Research, no. 6, Pags. 773-782, 1976.

López Garello, C.M., *Análisis Microestructural de la Fractura del Hormigón Utilizando Elementos Tipo Junta*. Aplicación a diferentes Hormigones. Tesis doctoral, Universitat Politécnica de Catalunya, Barcelona, España, 1999.

Lorefice, R., Etse, G., C.M. Lopez and I. Carol, *Mesomechanic Analysis of Time Dependent Concrete Behavior*. *EURO-C 2006,* Computational Modelling of Concrete Structures. Mayrhofen, Austria, 2006.

Lorefice, R., Etse, G., Rizo Patron, M., *Influencia de la Tasa de Deformación en el Creep y Relajación de Hormigones Normales*. ENIEF 2007, Córdoba, Argentina. Mecanica Computacional, Vol XXVI, 2007.

Lorefice, R., *Modelación de la Respuesta Dinámica del Hormigón Mediante los Criterios Meso y Macromecánicos*. Tesis Doctoral, CEMNCI - Univ. Nac. De Tucuman, 2007.

Lorefice, R., Etse, G., and Carol, I., *Viscoplastic Approach for Rate-Dependent Failure Analysis of Concrete Joints and Interfaces*. International Journal of Solids and Structures 45, 2686–2705, 2008.

Lorefice, R., Etse, G., Rizo Patron, M., *Integrated Analysis of Time Dependent Failure Using a Viscoplastic Theory*. ENIEF 2008, San Luis, Argentina, 2008. Publicado en Mecanica Computacional, Vol. XXVII, 2008.

Perzyna, P., The Constitutive Equations for Rate Sensitive Materials. *Quarter of Applied Mathematics*, Vol. 20, pp. 321-332, 1963.

Perzyna, P., Fundamental Problems in Viscoplasticity. *Advances in Applied Mechanics 9*, pp. 244-368, 1966.

Ponthot, J.P., Radial Return Extensions for Viscoplasticity and Lubricated Friction. *Proc. International Conference on Structural Mechanics and Reactor Technology SMIRT-13*. Porto Alegre, Brazil, Vol. 2, pp. 711-722, 1995.

Simo, J.C., Hughes, T.J.R., Elastoplasticity and Viscoplasticity. Computational aspects. *Springer-Verlag*, Berlin, 1998.

Sluys, J.L., Wave Propagation and Dispersion in Softening Solids. *PhD Thesis, TU-Delft*. The Netherlands, 1992.

Suaris, W., Shah, S. Rate-sensitive damage theory for brittle solids. Journal of Engineering Mechanics, ASCE 6 (110), 985–997, 1984.

Suaris, W., Shah, S. A constitutive model for concrete under dynamic loading. Journal of Structural Engineering, ASCE 111 (3), 563–576, 1985.

S. Tandon, K.T. Faber, Z. P. Bazant, and Y.~N. Li, Cohesive crack modeling of influence of sudden changes in loading rate on concrete fracture, Engrg. Fracture Mechanics, no. 52(6), pags. 987-997, 1995.

Wang, W.M., Stationary and Propagative Instabilities in Metals-A Computational Point of View". *PhD Thesis. TU-Delft*. The Netherlands, 1997.

Wang, W.M., Sluys, L.J., de Borst, R., Viscoplasticity for instabilities due to strain softening and strain-rate softening. *International Journal for Numerical Methods in Engineering*, 40, 3839-3864, 1997.

Willam, K. Etse, G. Munz, T., Localized Failure in Elastic - Viscoplastic Materials. *Proc. Concreep 5*, Barcelona, Ed. Z. P. Bazant and I. Carol, F. N. Spon, London, pp. 327-344, 1993.